HHS Public Access

Author manuscript

Heart Rhythm. Author manuscript; available in PMC 2018 September 01.

Published in final edited form as:

Heart Rhythm. 2017 September ; 14(9): 1406–1416. doi:10.1016/j.hrthm.2017.05.026.

QRS/T-Wave and Calcium Alternans in a Type I Diabetic Mouse Model for Spontaneous Post Myocardial Infarction Ventricular Tachycardia: A Mechanism for the Antiarrhythmic Effect of Statins

Hongwei Jin, PhD[1,2,*], **Charles M. Welzig, MD**[1,3,*], **Mark Aronovitz, BA**[1,2], **Farzad Noubary, PhD**[1,4], **Robert Blanton, MD**[1,2,5], **Bo Wang, MD**[1,2], **Mohammad Rajab, MD**[2,6], **Alfred Albano, MD**[1,2,7], **Mark S. Link, MD, FHRS**[1,4,8], **Sami F. Noujaim, PhD**[1,2,9], **Ho-Jin Park, PhD**[1,2], and **Jonas B. Galper, MD, PhD**[1,2,5]

[1]Tufts Medical Center, Tufts University School of Medicine, Boston, MA

[2]Molecular Cardiology Research Institute, Tufts Medical Center, Boston, MA

[3]Departments of Neurology, Physiology and Biomedical Engineering, Medical College of Wisconsin, Milwaukee, WI

[4]Tufts Clinical and Translational Science Institute, Tufts Medical Center, Boston, MA

[5]Cardiovascular Division, Cardiovascular Center, Department of Medicine, Tufts Medical Center, Boston, MA

[6]Department of Internal Medicine, Virginia Commonwealth University Medical Center, Richmond, VA

[7]Spectrum Health, Grand Rapids, MI

[8]UT Southwestern Medical Center, Dallas, TX

[9]Department of Molecular Pharmacology and Physiology, Morsani College of Medicine, Tampa, FL

Abstract

Background—The incidence of sudden arrhythmic death is markedly increased in diabetics.

Objective—Develop a mouse model for Post MI VT in the diabetic heart and determine the mechanism of an antiarrhythmic effect of statins.

Correspondence to: Hongwei Jin HJin@tuftsmedicalcenter.org, Ho-Jin Park HPark@tuftsmedicalcenter.org, Jonas B. Galper JGalper@tuftsmedicalcenter.org Molecular Cardiology Research Institute, Tufts Medical Center, 750 Washington St. Boston, MA 02111, USA. Tel.: 1-617-636-900(3)4, Fax: 1-617-636-4833.

*Drs. Jin and Welzig contributed equally to this work.

None of the authors has a conflict of interest.

Methods—EKG transmitters were implanted in wild type (WT), placebo and pravastatin treated Type I diabetic Akita mice, MIs induced by coronary ligation, Ca^{2+} transients studied by optical mapping, Ca^{2+} transients and sparks in left VM (VM) by the Ionoptix system and confocal microscopy.

Results—Burst pacing of Akita mouse hearts resulted in rate related QRS/T-Wave alternans, which was attenuated in pravastatin treated mice. Post MI Akita mice developed QRS/T-wave alternans and VT, 2,820 ± 879 beats/mouse which decreased to 343 ± 115 in pravastatin treated mice, (n=13, $P<0.05$). Optical mapping demonstrated pacing induced VT originating in the peri-infarction zone and Ca^{2+} alternans, both attenuated in hearts of statin treated mice. Akita VM displayed: Ca^{2+} alternans, triggered activity, increased; Ca^{2+} transient decay time (Tau), incidence of Ca^{2+} sparks and cytosolic Ca^{2+} and decreased SR Ca^{2+} stores which were in part reversed in cells from statin treated mice. Homogenates of Akita ventricles demonstrated decreased SERCA2a/PLB ratio and increased ratio of protein phosphatase (PP-1) to the PP-1 inhibitor PPI-1 reversed in homogenates of pravastatin treated Akita mice.

Conclusions—Pravastatin decreased the incidence of post MI VT and Ca^{2+} alternans in Akita mouse hearts in part via the reversal of abnormalities of Ca^{2+} handling via the PP-1/PPI-1 pathway.

Keywords

QRS/T-Wave alternans; Ca^{2+} alternans; ventricular tachycardia; diabetes; myocardial infarction; statins; Ca^{2+} handling proteins; Akita mouse

Introduction

QRS/T-wave alternans, a rate dependent beat to beat fluctuation in the surface electrocardiogram, has been associated with life threatening ventricular arrhythmias[1] and sudden death in the setting of MI, long QT syndrome, and heart failure[2]. T-wave alternans on the surface EKG is felt to reflect events occurring at the single myocyte level and has been attributed to either a temporal or spatial dispersion of myocyte repolarization or abnormalities of Ca^{2+} cycling[3,4]. Ca^{2+} alternans, defined as alternating oscillations in the amplitude of Ca^{2+} transients, which may be manifested as variations in contractility, has been closely linked to the pathogenesis of VT and sudden death in heart failure[5]. Alternans due to dysfunctional Ca^{2+} cycling may reflect the inability of the myocyte to cycle Ca^{2+} beat to beat in response to increasing heart rate and has been attributed to abnormalities in the function of Ca^{2+} handling proteins[6–8]. Studies in the diabetic heart carried out mainly in streptozotocin (STZ) and/or alloxan induced diabetic rats or dogs have suggested that diabetes is associated with abnormalities of Ca^{2+} handling[9]. No direct correlation to the development of ventricular arrhythmia and sudden death in diabetes has been demonstrated.

Although statins may have an antiarrhythmic benefit in the setting of MI via a reduction in ischemic burden, a reduction in arrhythmic death and a decrease in appropriate implantable cardiac defibrillator firing have been reported in patients with both ischemic and non-ischemic cardiomyopathy[10] consistent with the hypothesis that statins might have a direct antiarrhythmic effect. Here we use the Akita Type I diabetic mouse, characterized by a point

mutation in the pro-insulin gene which interferes with insulin processing, as an animal model for the study of the mechanism of post MI arrhythmias in the diabetic heart and the mechanism of the antiarrhythmic effect of statins in these mice[11,12]. We demonstrated that these mice develop QRS/T-Wave alternans and VT in response to burst pacing, which was attenuated by pravastatin treatment[12]. We further determined that these mice develop VT in the setting of acute MI, the role of Ca^{2+} -dyshomeostasis in the pathogenesis of VT and the therapeutic effect of pravastatin.

Methods

Animals

Akita type I diabetic mice (C57BL/6J-$Ins2^{Akita}$ were obtained from Jackson Laboratories (See Supplemental data). For pravastatin treatment, Akita mice were treated for 7 days with either pravastatin 20mg.$kg^{-1}day^{-1}$ IP or an equal volume of normal saline, placebo. The dose of pravastatin was based on observations comparing dose and blood levels in mice and patients[13, 14]. All vertebrate animal-related procedures described here were approved by the Tufts Medical Center Institutional Animal Care Committee.

Coronary Artery ligation

EKG transmitters (DSI) were implanted. Telemetry data were recorded for a 1-hour baseline prior to coronary artery ligation and continuously for 30 hours post MI. Recordings were analyzed using a ventricular arrhythmia detector and classifier implemented by custom built software. The beginning and end of each occurrence of PVCs, doublets and triplets, non-sustained and sustained (≥3 seconds duration) VT, as well as the number of arrhythmic beats involved for each event was documented and visually verified. Results were derived from the incidence of runs of 3 or more consecutive beats during non-sustained and sustained VT. “VT beats” refers to the number of such beats observed.

Echocardiography

Echocardiographic studies were performed using a VisualSonics Vivo 2100 as described[15].

Optical imaging of Calcium transients

Ca^{2+} transients optical mapping was carried as described[12]. Rhod-2 AM (0.4–0.6mL of 1mg/mL solution in DMSO, Invitrogen, Carlsbad, CA) was used as a Ca^{2+} indicator.

Cell isolation and electrophysiologic measurements

Dissociated VM from mouse left ventricles were prepared as described[16]. L-type Ca^{2+} currents, Ca^{2+} transients and Ca^{2+} spark recordings were carried out as indicted (supplemental data)[17,18].

Immunoblotting

Protein extracts were prepared, and immunoblotting was performed as described[16]. Primary antibodies (Supplemental data).

Statistical analysis

Average values are expressed as means ± SEM. Statistical differences between mean values calculated by Student's *t*-test or Mann-Whitney *U*-test as appropriate (two sided). The significance of differences between the incidence and frequency of events was calculated by the Pearson Chi-Square test or Likelihood Ratio. For cellular alternans, a mixed-effects logistic regression model was fitted to assess the association between the binary outcome of stimulation response alternans and categorical covariates: stimulation frequency, type of mouse (WT vs. Akita), and treatment (placebo vs. pravastatin). The model included a random intercept to account for the correlation between multiple tissue samples from the same mouse.

Results

QRS/T-Wave alternans in response to burst pacing in the Akita mouse heart

We previously demonstrated that the Akita Type I diabetic mouse is markedly inducible for VT in response to programmed ventricular stimulation, and that inducibility was significantly attenuated in Akita mice pretreated with pravastatin[12]. Further analysis of the surface EKG in these mice demonstrated a rate related beat to beat alteration in the surface and intracardiac ECG (Fig. 1A, C) consistent with QRS/T-Wave alternans (Fig. 1B, D), preceded the development of runs of VT, non-sustained VT (NSVT) and ventricular flutter (Fig. 1E). At a pacing rate of 1000bpm alternans was observed in 7/14 Akitas, 9/16 placebo treated Akitas and 0/14 WT mice ($p<0.006$ and 0.001, respectively vs WT by Fischer's-exact test). At 1250bpm, 12/14 Akitas, 14/16 placebo treated Akitas and 3/14 WT ($p<0.001$ and 0.001, respectively vs WT, χ^2) and only 9/19 statin treated Akitas developed alternans ($p=0.013$ vs placebo, χ^2). Given that mice were subjected to successively increasing pacing rates, one limitation of these data is the potential carry over effect from the prior pacing rate.

The Akita mouse as a model for post MI VT in Type I diabetes

Given the relationship between QRS/T-Wave alternans and the predisposition to ventricular arrhythmia[1] in the setting of MI, we determined whether Akita mice developed VT following acute MI. All mice demonstrated ST elevation (Fig. 2A, B). 10/14Akita mice developed QRS/T-wave alternans following coronary artery ligation (Fig. 2B). Subsequently, these mice developed increasing ventricular irritability progressing from PVCs. couplets, to longer runs of NSVT, and sporadic runs of VT (See Fig. 2C, D, E). Interestingly, heart rates following MI were not significantly different from those observed prior to MI. A plot of hourly sums of VT beats (i.e. runs of three or more beats) for all placebo treated Akita mice demonstrates an initial phase peaking at 10 to 14h post MI and a second phase from 18–28 hours; the latter demonstrating longer runs of both NSVT and VT (Fig. 2F). The mean number of VT beats/mouse was 2,820 ± 879 in placebo treated mice and the average total duration of VT beats was 200 ± 65 sec (n= 12). WT mice demonstrated only occasional PVCs (n=4, Fig. 2G, H).

Pravastatin attenuates the incidence of Post MI VT in the Akita mouse

Compared with placebo, the mean number of VT beats in pravastatin treated mice decreased to 343 ± 115 (n=13, $P<0.05$, Fig. 2G) and average total duration of VT to 22.1±7.7s ($P<0.05$) Fig. 2H. Interestingly, the late phase VT was absent in pravastatin treated mice, Fig. 2F.

Comparison of infarct size and area at risk

Echocardiographic analysis demonstrated no significant differences in infarct size, ejection fraction, chamber size and fractional shortening (Supplemental Table SI). Infarct size and area at risk by Evans blue injection and TCC staining respectively were also not significantly different (P≤0.05, Supplemental Fig. S1 A–C).

Ca^{2+} alternans and MI in Akita mice

Optical mapping demonstrated that infarcted hearts from placebo treated Akita mice, harvested at the peak of spontaneous VT, developed runs of VT originating in the peri-infarct zone in response to burst pacing, while WT hearts did not (Fig. 3A, lower panel, Fig. 3B). Hearts from placebo treated mice developed Ca^{2+} alternans in both the peri-infarction zone Fig. 3C and remote myocardium (data not shown), with an alternans ratio of 0.713±. 009 (n=3) and threshold between 9–12Hz (Fig. 3E). Hearts from WT mice did not develop alternans at these pacing rates. Hearts from pravastatin treated mice displayed neither pacing induced VT nor Ca^{2+} alternans in either the peri-infarction zone or remote myocardium, alternans ratio of 1.010±0.030 (n=3, $P<0.01$) Fig. 3D, E. Interestingly, neither action potential (AP) alternans nor repolarization alternans could be demonstrated and there was no evidence of spatially discordant alternans in Akita hearts at these pacing rates.

Pravastatin increases the threshold for calcium alternans in VM from Akita mice

Five-percent of VM (n=20) from WT mice demonstrated an alternans threshold averaging 4 Hz and a maximum response at 5Hz (Fig. 4A, D), 14/23, (60.9 %) of VM from placebo treated Akita mice exhibited Ca^{2+} alternans with a threshold of 1Hz and a maximal response >4 Hz, Fig. 4B, D and 29.2% (7/24) VM from statin treated mice developed alternans at 3Hz compared with 60.9% (14/23, $P<0.05$) of cells from placebo treated mice (Fig. 4D). The estimated odds ratios (OR) and their 95% confidence intervals (CI) from the mixed-effects logistic regression model are shown in Table S2. All three categorical covariates (stimulation frequency, type of mouse, and treatment) were highly significant predictors of response to stimulation with alternans (p-value < 0.0001). These cells also demonstrated mechanical alternans in response to increased rates of field stimulation measured using video motion detector software (supplemental Fig. S2).

Triggered activity in is attenuated in VM from pravastatin treated Akita mice

Perfusion of VM paced at 1Hz with 100 nmol/L ISO, had no effect on triggered activity in cells from WT mice (n=14), compared with 79% (11 of 14) cells from Akita (P<0.01) and 23.1% (3 of 13) in cells from pravastatin treated Akita mice ($P<0.01$ compared to Akita, Fig. 4E–H).

Ca^{2+} alternans in Akita VM is associated with decreased SR Ca^{2+}

Fluctuations and/or depletion of sarcoplasmic reticulum (SR) Ca^{2+} have been reported to play an important role in the development of Ca^{2+} alternans[19]. SR Ca^{2+} content was significantly decreased in cells from Akita mice (0.26 ± 0.04, n=16) compared with WT (0.42 ± 0.04, n=14, P<0.01), but was increased (0.37±0.02, n=12, P<0.05, compared with Akita) in cells from statin treated Akita mice, Fig. 5A–D.

SR Ca^{2+} depletion in VM from Akita mice and increased RyR2 leak

We determined whether the decrease in SR Ca^{2+} content reflected increased SR Ca^{2+} leak. The frequency of spontaneous Ca^{2+} sparks was significantly different in myocytes from WT, Akita and pravastatin treated Akita mice: 6.72 ± 0.85 (n=23), 19.7 ± 1.48 (n=36) and 12.0±1.41 (n=33) sparks/100μm/s, respectively (Fig. 6A, C). The mean amplitude of Ca^{2+} sparks was 1.52 ± 0.36 (n=27) in WT *vs* 0.66 ± 0.03 (n=36) in Akita myocytes (P<0.01) and increased to 0.97±0.06 in the statin treated group (n=33, P<0.01 compared to Akita, Fig. 5D) consistent with the decreased levels of SR Ca^{2+} in these cells. These findings are further supported by measurements of SR RYR_2 leak: 7.2±1.8% (n=14) in WT vs. 19.2±2.5% in Akita myocytes (n=15, P<0.001), and 12.2±1.7% in myocytes from pravastatin treated Akita mice (n=10) P<0.05 compared to cells from placebo treated mice, Fig. 5A–C, E. SR Ca^{2+} depletion correlated with RyR_2 leak, R^2=0.5065, p<0.0001.

Ca^{2+} reuptake was decreased in VM from Akita mice

Comparison of representative traces of Ca^{2+} transients demonstrated a similar upstroke and peak height for all 3 groups (Fig. 7A). However, the mean value for tau, the slope of the recovery phase, was increased in cells from Akita compared with WT mice 0.17 ± 0.01 (n=23) vs. 0.14 ± 0.01, n=20 (P< 0.05), but decreased to 0.15 ±0.01, n=28, in myocytes from pravastatin treated mice (P<0.05 compared with Akitas, Fig. 7A, B, C). Sarcomere shortening was not significantly different in all 3 groups, data not shown.

Cytosolic Ca^{2+} is increased in VM from Akita mice, while L-Type Ca^{2+} currents are unchanged

Cytosolic Ca^{2+} in VMs from replicate measurements of Ca^{2+} transients were significantly elevated in Akita mice vs. WT; 0.22±0.02μM vs. 0.11±0.02μM (n=15, P<0.01) and decreased to 0.18±0.01μM (n=15) in cells from pravastatin mice (P<0.01 compared to Akita, Fig. 7D). Increased cytosolic Ca^{2+} in VM from Akita mice might reflect an increase in L-Type Ca^{2+} currents. Peak Ca^{2+} current densities and current voltage relationships were similar in both VM WT and Akita mice (Supplemental Fig. S3). Furthermore, there was no significant difference in expression of the Cav1.2, Na^+/Ca^{2+} exchanger, NCX, RyR_2 and p2808RyR_2 in ventricular extracts from these mice (Supplementary Fig. S4 A–C).

The changes in Ca^{2+} handling proteins in the Akita ventricles are partially reversed by pravastatin

To determine the mechanism of decreased SR Ca^{2+} reuptake, we measured levels of Ca^{2+} handling proteins. While SERCA2a levels were unchanged, t-PLB was increased 1.37±0.05 fold (n=3, P<0.01) vs WT and decreased to 0.91±0.10 (n=3, P<0.05) fold compared to WT

in extracts of placebo and pravastatin treated Akitas respectively, Fig. 8A–C. Hence the ratio of SERCA2a/t-PLB was 2.28±0.09 in WT extracts vs 1.70±0.06 (n=3, P<0.01) in Akita and 2.61±0.33(n=3) in pravastatin treated Akitas (P<0.05, compared with Akita, Fig. 8A–D). Given that unphosphorlyated PLB inhibits SERCA-2A activity, we compared the levels of pSer16-PLB and pThr17-PLB. pSer16-PLB and pThr17-PLB were decreased 0.67±0.03 fold (n=3, P<0.05) and 0.33±0.03 fold respectively (n=3, P<0.05) in Akita mice compared with WT, but was decreased only 0.96±0.07fold (n=3, P<0.05) and 0.66±0.07fold (n=3, P<0.05) compared to WT in ventricles of pravastatin treated mice (Fig. 8A, E, F).

Given the role of PP-1 in the dephosphorylation of PLB, we determined the levels of PP-1 and it inhibitor PPI-1. PP-1 was increased 2.34±0.06 fold (n=3, P<0.01) in Akita ventricles compared with WT and 1.60±0.18fold (n=3) in homogenates of pravastatin treated Akitas (P<0.05, Fig. 8G, J) with a reciprocal change in PP-1, (Fig. 8G, I). Hence the ratio of PP-1/PPI-1 in Akita was 6.79±0.17 fold higher (n=3, P<0.05) compared with WT, and decreased to 0.51±0.06 fold (n=3, P<0.01) in pravastatin treated Akita mice compared with Akita, (Fig. 8K). Given that PPI-1 activity has also been shown to be negatively regulated by PKCα mediated phosphorylation at Ser67, we next determined the level of pSerPPI-1[20]. pSer67PPI-1 was increased 3.76±0.36 fold (n=3, P<0.01) in Akita ventricles compared with WT and 1.43±0.35 fold (n=3) above WT in ventricles of pravastatin treated Akitas, P<0.05 (Fig. 8G, H). Finally, we determined whether increased pSer67PPI-1 might reflect increased PCKα activity in the Akita heart. PKCα activity, measured as translocation from the cytosol to the membrane demonstrated a 0.42±0.03 fold (n=4, P<0.05) decrease in the cytosolic form in extracts of Akita ventricles compared with WT, and a reciprocal 1.41±0.04fold increase (n=3, P<0.05) in the membrane associated form which was in part reversed in extracts of statin treated mice consistent with a role of increased PKCα activity in the inactivation of PP-1 by increased phosphorylation at Ser67, Fig. 8L, M, N.

Discussion

Here we develop the Akita mouse as a new animal model for the study of the mechanism and treatment of post MI VT in the Type I diabetic heart. This mouse demonstrates QRS/T-wave alternans in response to burst pacing and coronary artery ligation, which was attenuated in pravastatin treated mice. Significant data support the conclusion that T-wave alternans reflects action potential duration(APD) alternans occurring at the single myocyte level, which when combined with QRS alternans reflecting conduction velocity alternans at the tissue level, produces temporal and spatial dispersion of repolarization resulting in a high probability of reentrant arrhythmias[1,8]. T-Wave alternans may be related to APD alternans caused by steep restitution (the relationship between the action potential duration of one beat and the diastolic interval of the proceeding beat)[3] or secondary to Ca^{2+} alternans[8]. Ca^{2+} recycling abnormalities promoting Ca^{2+} alternans are commonly associated with ischemia, MI and heart failure[4,5]. These data are consistent with our finding that following coronary artery ligation, Akita mice demonstrate QRS/T wave alternans without a significant change in heart rate consistent with an increased propensity of the heart to develop alternans in the setting of MI[21]. These same abnormalities can concurrently predispose cardiac myocytes to spontaneous diastolic SR Ca^{2+} release resulting in delayed afterdepolarization-related triggered activity[22].

Furthermore, hearts from Akita mice developed rate related Ca^{2+} transient alternans and increased susceptibility of cardiomyocytes to isoproterenol-induced triggered activity, both of which were attenuated in pravastatin pretreated mice. These factors are known to predispose to arrhythmia and sudden death in the settings of heart failure and ischemia[23], but had not been previously demonstrated in the diabetic heart.

Although we noted that increased susceptibility to rapid pacing induced QRS/T-Wave alternans in the surface ECG and in the intracardiac electrogram of the Akita mouse, consistent with underlying arhythmogenic spatially discordant repolarization alternans, we did not observe spatially discordant APD alternans during optical mapping of action potentials recorded from multiple epicardial sites[1]. This could indicate that the QRS/T-Wave alternans arose primarily from the endocardial or midmyocardial layers and were not detected on the epicardial surface. Alternatively, the cause of ventricular arrhythmias in the Akita mice during the post infarction period may be more related to triggered activity than spatially discordant alternans, consistent with the observation of the focal origin of VT revealed by optical mapping. In either case the data support that Ca^{2+} cycling is abnormal in Akita mice and resembles changes seen in heart failure, with down regulation of SERCA and increased RyR_2 leakiness that are known to promote both Ca^{2+} alternans and spontaneous SR Ca^{2+} release underlying triggered activity[22].

Specifically, studies demonstrated depletion of SR Ca^{2+} and increased cytosolic Ca^{2+} associated decreased Ca^{2+} reuptake by the SR during diastole and increased SR Ca^{2+} leak which were reversed in part in cells from pravastatin treated mice. Studies of the mechanism of decreased Ca^{2+} reuptake demonstrated a decrease in the ratio of SERCA-2a/PLB and p-PLB, which were at least in part reversed in ventricular extracts of pravastatin treated Akita mice. Furthermore, dephosphorylation of PLB was associated with increased PP-1 and decreased in both PPI-1 expression and activation which were reversed by statins. Although changes in PP-1/PPI-1 have been suggested in failing hearts[24], our data are the first to demonstrate a reciprocal relationship between PP1 and PPI-1 in the diabetic heart. These data offer strong support for a unique mechanism by which pravastatin attenuates the development of Ca^{2+} alternans and the predisposition to Post MI VT in the Akita mouse heart in part by reversing the hyperactivity of the PKCα/PPI-1 pathway thus attenuating the depletion of SR Ca^{2+} and the increase in cytosolic Ca^{2+} and restoring Ca^{2+} homeostasis.

It should be noted that the interpretation of these data are limited by differences in resting heart rate and mechanisms of repolarization in the mouse compared with large mammals.

Conclusions

The finding that the anti-arrhythmic effect of pravastatin is associated with the attenuation of QRS and T-Wave alternans, Ca^{2+} transient alternans, an increase in SR Ca^{2+} reuptake, and a reversal of the PP-1/PPI-1 ratio, offers further insight into the PKCα/PP-1/PPI-1 pathway as a therapeutic target in the treatment and prevention of post MI VT in Type I diabetes.

Supplementary Material

Refer to Web version on PubMed Central for supplementary material.

Acknowledgments

Work was supported by NIH grants R01HL074876 and R01HL087827 to JBG and R21DK079622 to HP and the NIH CTSA award UL1TR001064 and the AHA grant 13SDG17050021 to HJ. We would like to acknowledge Dr. James Weiss for his reading and discussion of the manuscript and invaluable and insightful comments.

References

1. Pastore JM, Girouard SD, Laurita KR, Akar FG, Rosenbaum DS. Mechanism linking T-wave alternans to the genesis of cardiac fibrillation. Circulation. 1999; 99:1385–94. [PubMed: 10077525]
2. Cutler MJ, Rosenbaum DS. Explaining the clinical manifestations of T wave alternans in patients at risk for sudden cardiac death. Heart Rhythm. 2009; 6:S22–8. [PubMed: 19168395]
3. Narayan SM. T-wave alternans and the susceptibility to ventricular arrhythmias. J Am Coll Cardiol. 2006; 47:269–81. [PubMed: 16412847]
4. Verrier RL, Malik M. Electrophysiology of T-wave alternans: mechanisms and pharmacologic influences. J Electrocardiol. 2013; 46:580–4. [PubMed: 23948521]
5. Laurita KR, Rosenbaum DS. Cellular mechanisms of arrhythmogenic cardiac alternans. Prog Biophys Mol Biol. 2008; 97:332–347. [PubMed: 18395246]
6. Diaz ME, O'Neill SC, Eisner DA. Sarcoplasmic reticulum calcium content fluctuation is the key to cardiac alternans. Circ Res. 2004; 94:650–6. [PubMed: 14752033]
7. Picht E, DeSantiago J, Blatter LA, Bers DM. Cardiac alternans do not rely on diastolic sarcoplasmic reticulum calcium content fluctuations. Circ Res. 2006; 99:740–8. [PubMed: 16946134]
8. Qu Z, Nivala M, Weiss JN. Calcium alternans in cardiac myocytes: order from disorder. J Mol Cell Cardiol. 2013; 58:100–9. [PubMed: 23104004]
9. Choi KM, Zhong Y, Hoit BD, Grupp IL, Hahn H, Dilly KW, Guatimosim S, Lederer WJ, Matlib MA. Defective intracellular Ca(2+) signaling contributes to cardiomyopathy in Type 1 diabetic rats. Am J Physiol Heart Circ Physiol. 2002; 283:H1398–408. [PubMed: 12234790]
10. Das MK, Zipes DP. Antiarrhythmic and nonantiarrhythmic drugs for sudden cardiac death prevention. J Cardiovasc Pharmacol. 2010; 55:438–449. [PubMed: 20509177]
11. Kayo T, Koizumi A. Mapping of murine diabetogenic gene Mody on chromosome 7 at D7Mit258 and its involvement in pancreatic islet and β cell development during the perinatal period. J Clin Invest. 1998; 101:2112–2118. [PubMed: 9593767]
12. Rajab M, Jin H, Welzig CM, Albano A, Aronovitz M, Zhang Y, Park HJ, Link MS, Noujaim SF, Galper JB. Increased inducibility of ventricular tachycardia and decreased heart rate variability in a mouse model for type 1 diabetes: Effect of pravastatin. American Journal of Physiology - Heart and Circulatory Physiology. 2013; 305:H1807–H1816. [PubMed: 24163078]
13. Johnson J, Carson K, Williams H, Karanam S, Newby A, Angelini G, George S, Jackson C. Plaque rupture after short periods of fat feeding in the apolipoprotein E-knockout mouse: model characterization and effects of pravastatin treatment. Circulation. 2005; 111:1422–30. [PubMed: 15781753]
14. Yao HW, Mao LG, Zhu JP. Protective effects of pravastatin in murine lipopolysaccharide-induced acute lung injury. Clinical and experimental pharmacology & physiology. 2006; 33:793–7. [PubMed: 16922808]
15. Zhang Y, Welzig CM, Picard KL, et al. Glycogen synthase kinase-3β inhibition ameliorates cardiac parasympathetic dysfunction in type 1 diabetic akita mice. Diabetes. 2014; 63:2097–2113. [PubMed: 24458356]
16. Park HJ, Zhang Y, Du C, et al. Role of SREBP-1 in the development of parasympathetic dysfunction in the hearts of type 1 diabetic akita mice. Circ Res. 2009; 105:287–294. [PubMed: 19423844]
17. Shannon TR, Ginsburg KS, Bers DM. Quantitative assessment of the SR Ca2+ leak-load relationship. Circ Res. 2002; 91:594–600. [PubMed: 12364387]
18. Cheng H, Lederer WJ, Cannell MB. Calcium sparks: elementary events underlying excitation-contraction coupling in heart muscle. Science. 1993; 262:740–744. [PubMed: 8235594]

19. Díaz ME, O'Neill SC, Eisner DA. Sarcoplasmic Reticulum Calcium Content Fluctuation Is the Key to Cardiac Alternans. Circ Res. 2004; 94:650–656. [PubMed: 14752033]

20. Wittköpper K, Dobrev D, Eschenhagen T, El-Armouche A. Phosphatase-1 inhibitor-1 in physiological and pathological β-adrenoceptor signalling. Cardiovasc Res. 2011; 91:392–401. [PubMed: 21354993]

21. Chou CC, Zhou S, Hayashi H, et al. Remodelling of action potential and intracellular calcium cycling dynamics during subacute myocardial infarction promotes ventricular arrhythmias in Langendorff-perfused rabbit hearts. The Journal of physiology. 2007; 580:895–906. [PubMed: 17272354]

22. Weiss JN, Garfinkel A, Karagueuzian HS, Nguyen TP, Olcese R, Chen PS, Qu Z. Perspective: a dynamics-based classification of ventricular arrhythmias. J Mol Cell Cardiol. 2015; 82:136–52. [PubMed: 25769672]

23. Hsueh CH, Chen NX, Lin SF, Chen PS, Gattone VH, Allen MR, Fishbein MC, Moe SM. Pathogenesis of arrhythmias in a model of CKD. J Am Soc Nephrol. 2014; 25:2812–2821. [PubMed: 24854269]

24. Neumann J, Eschenhagen T, Jones LR, Linck B, Schmitz W, Scholz H, Zimmermann N. Increased expression of cardiac phosphatases in patients with end-stage heart failure. J Mol Cell Cardiol. 1997; 29:265–272. [PubMed: 9040041]

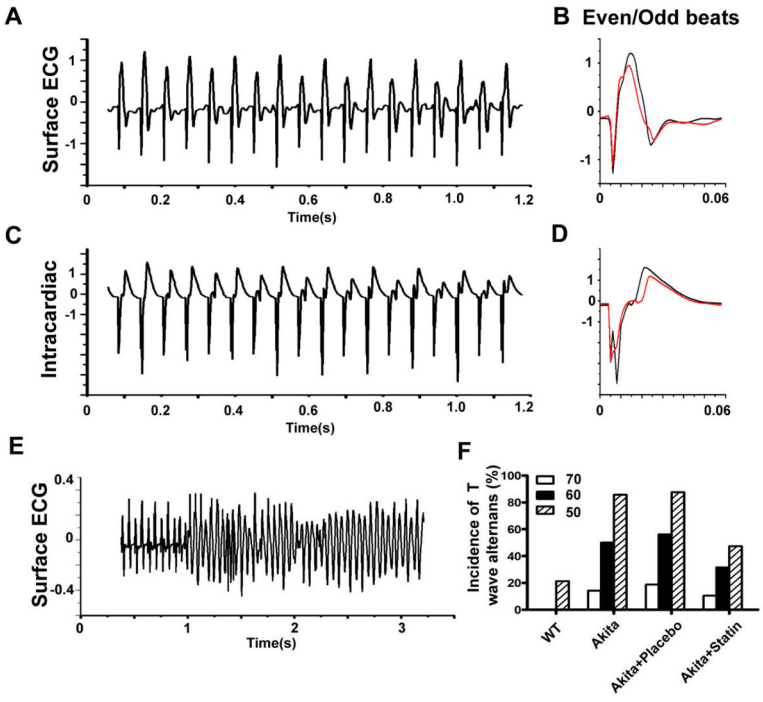

Figure 1.

The development of QRS/T-Wave alternans in response to burst pacing in the Akita mouse. Response to bust pacing at 1000 bpm on A. Surface ECG, C. Intracardiac electrogram; B and D: Averaged and superimposed even and odd beats from A and C. E. Surface EKG at pacing rate of 1000 bpm followed by a run of VF. F. Percent of WT, Akita, Statin and placebo treated Akita mice developing QRS/T-wave alternans at pacing intervals of 70, 60 and 50ms.

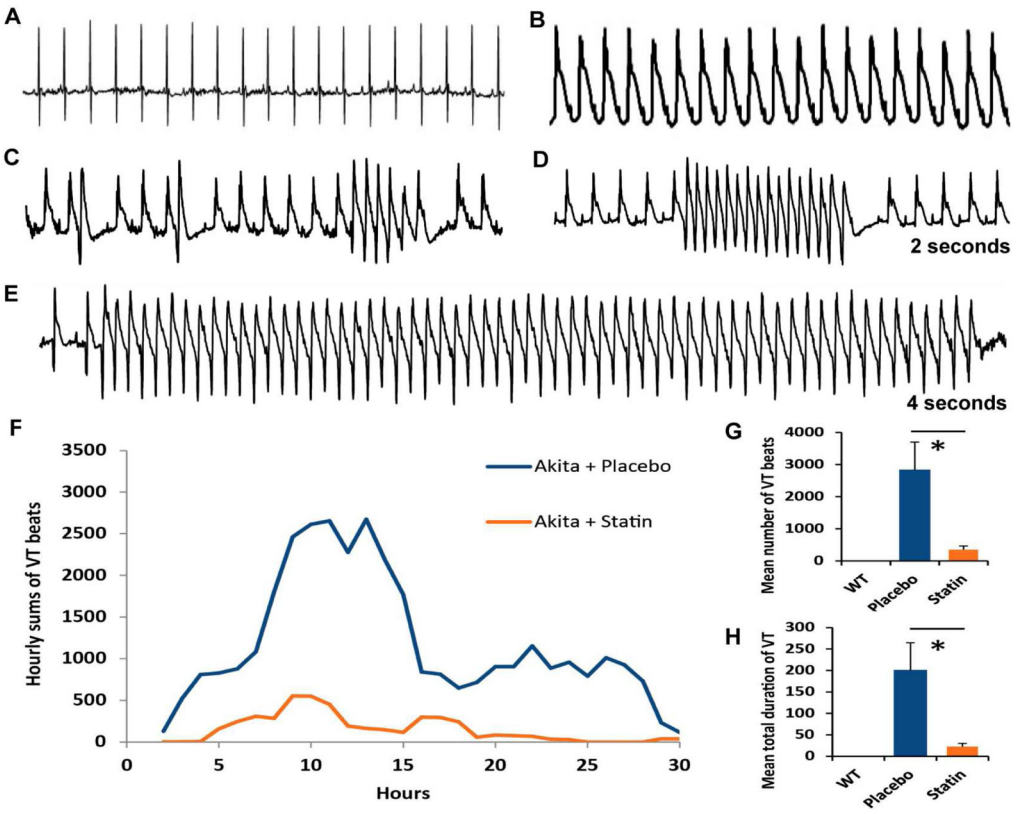

Figure 2.

The effect of pravastatin on post MI VT. Typical EKG A. prior to and B. immediately following coronary artery ligation. Note: QRS/T-wave alternans. Development of C. PVCs, doublets and triplets. D. NSVT and E. VT. F. Time course of the development of post-MI VT plotted as the 3-hour moving average of the hourly sums of VT beats in placebo vs statin treated Akita. Comparison of G: the mean number of VT beats; H. the mean total duration of VT events in WT, placebo and pravastatin treated Akita mice. **P*<0.05.

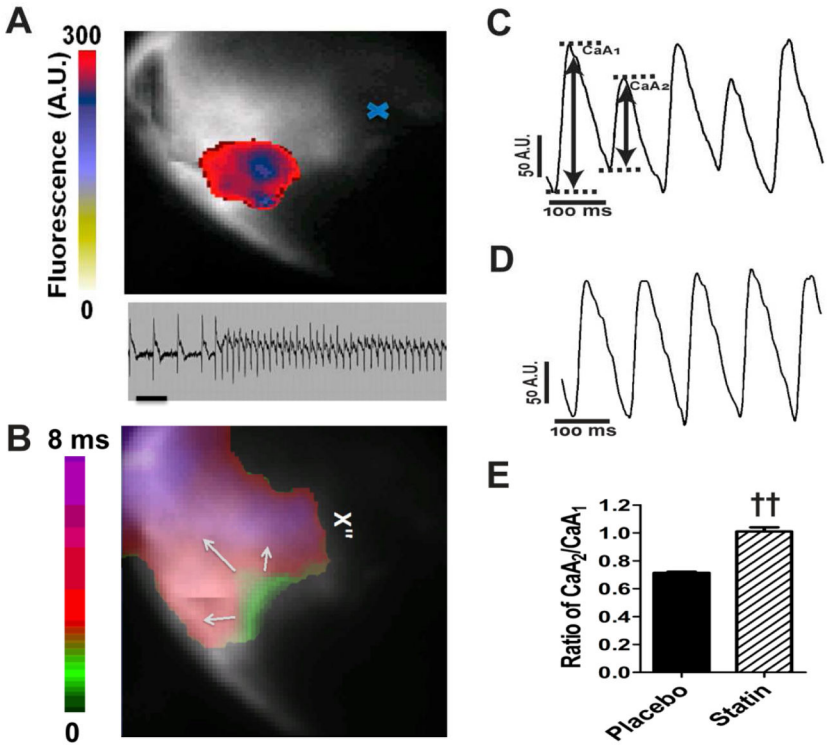

Figure 3.

Optical mapping of Ca^{2+} transient alternans in infarcted hearts from Akita mice. A. VT is focal, originating in the peri-infarct zone. The colored voltage fluorescence snapshot of the first tachyarrhythmic beat is superimposed on the fluorescence image of the heart. The scale indicates the fluorescence in arbitrary units, and the blue x indicates the location of the ligation site. Lower panel. The ECG is of the tachycardic episode mapped above. Scale bar: 200ms. B. Activation map demonstrating the initiation of VT in the peri-infarction zone. C. Ca^{2+} transients recorded from the peri-infarct zone 12 hours following coronary artery ligation in epicardially paced hearts at 12Hz from B. placebo treated and D. pravastatin treated Akita mice. E. Alternans ratio of Ca^{2+} transients in hearts from placebo and pravastatin treated mice defined as A_2/A_1. ††P<0.01 vs placebo.

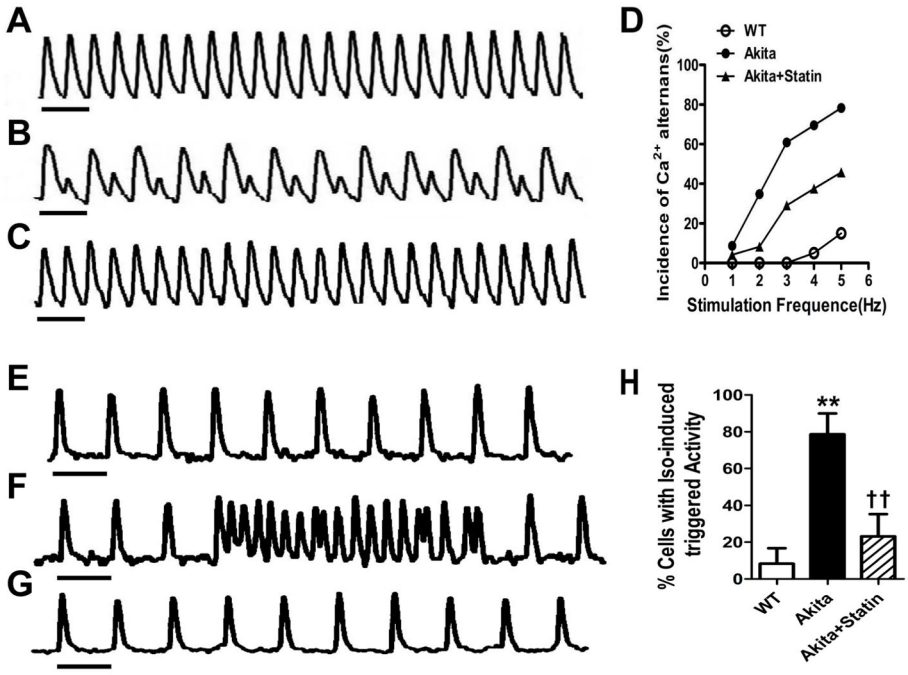

Figure 4.

Ca^{2+} alternans in VM from Akita mice is associated with triggered activity and is attenuated in pravastatin treated group. Representative Ca^{2+} transient trace paced at 3Hz from A: WT, B Akita and C Akita mice treated with pravastatin. D. Incidence of Ca^{2+} alternans in VM paced at 1–5 Hz. Isoproterenol stimulated triggered activity in VM from E. WT, F. Akita and G. pravastatin treated Akita mice. H.% of cells demonstrating ISO stimulated triggered activity. *0.05, **P<0.01 vs WT; †*P*<0.05, ††*P*<0.01 vs Akita. Horizontal bar:1 second.

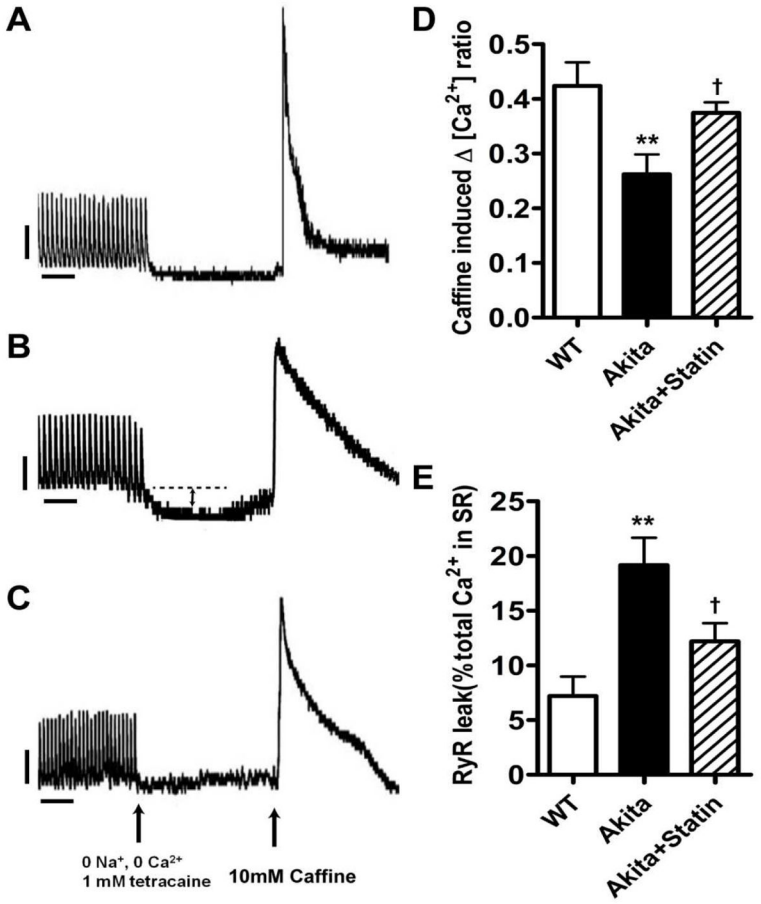

Figure 5.

Decreased SR Ca^{2+} content and increased SRCa^{2+} leak in VM from Akita mice are partially reversed in pravastatin treated Akitas. Cytosolic Ca^{2+} was determined in cells paced at 1 Hz for 20 sec followed by switching for 20 secs to 0 Na^{+} and 0 Ca^{2+} and 1mMol/L tetracaine to inhibit Na^{+} flux followed by 10mM caffeine. Ca^{2+} content was measured as the ratio of fluorescence at 340/380. Cells from A. WT. B. placebo treated Akita C. pravastatin treated mice, D. SR Ca^{2+} content, E. SR Ca^{2+} leak. Double headed arrow in B represents SR Ca^{2+} leak, Arrows in C represent time of switching of perfusion medium and addition of Caffeine. ** P<0.01 vs WT, † P<0.05 vs Akita. Vertical bar: 0.1, Horizontal bar: 5 seconds.

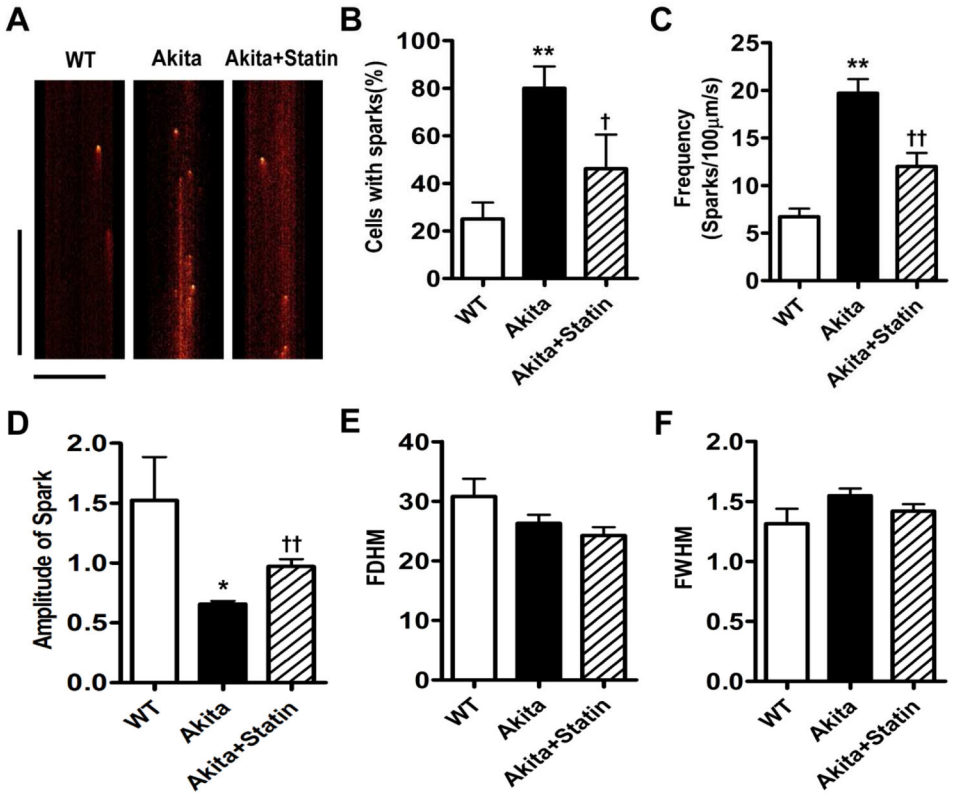

Figure 6.

Increased Ca^{2+} sparks in VM from Akita mice are attenuated in pravastatin treated mice. A. Line scan images. B. Percent of cells with sparks, C. Frequency of sparks, D. Amplitude of sparks, E. Full duration at half maximum amplitude (FDHM) and F. Full width at half maximum amplitude (FWHM). *P<0.05, **P<0.01 vs WT; †P<0.05, ††P<0.01 vs Akita. Vertical bar: 500 milliseconds, Horizontal bar: 20 μm.

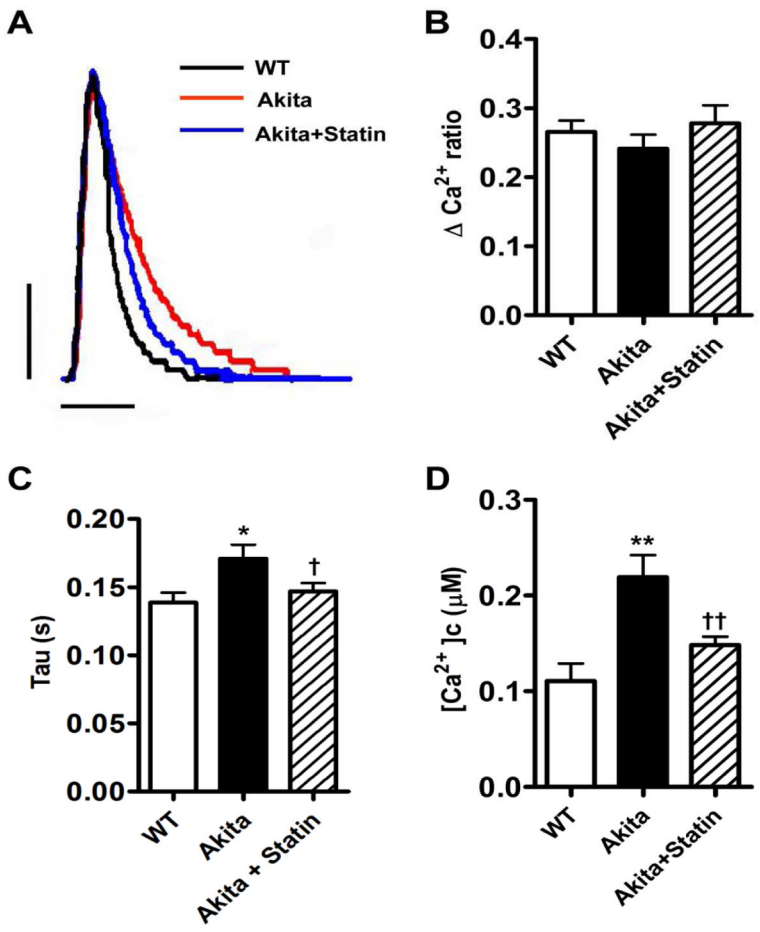

Figure 7.

Effect of pravastatin on SR Ca^{2+} reuptake and cytosolic free Ca^{2+} in VM from Akita mice. A. Representative superimposed Ca^{2+} transients VM from WT, Akita and pravastatin treated Akitas. B. Absolute peak height of Ca^{2+} transients, Δ Ca^{2+} ratio. C. Tau, time constant for Ca^{2+} reuptake, D. Cytosolic free Ca^{2+} concentration. **P*<0.05, ***P*<0.01 vs WT, †*P*<0.05, ††*P*<0.01 vs Akita. Vertical bar: 0.1, Horizontal bar: 0.2 millisecond.

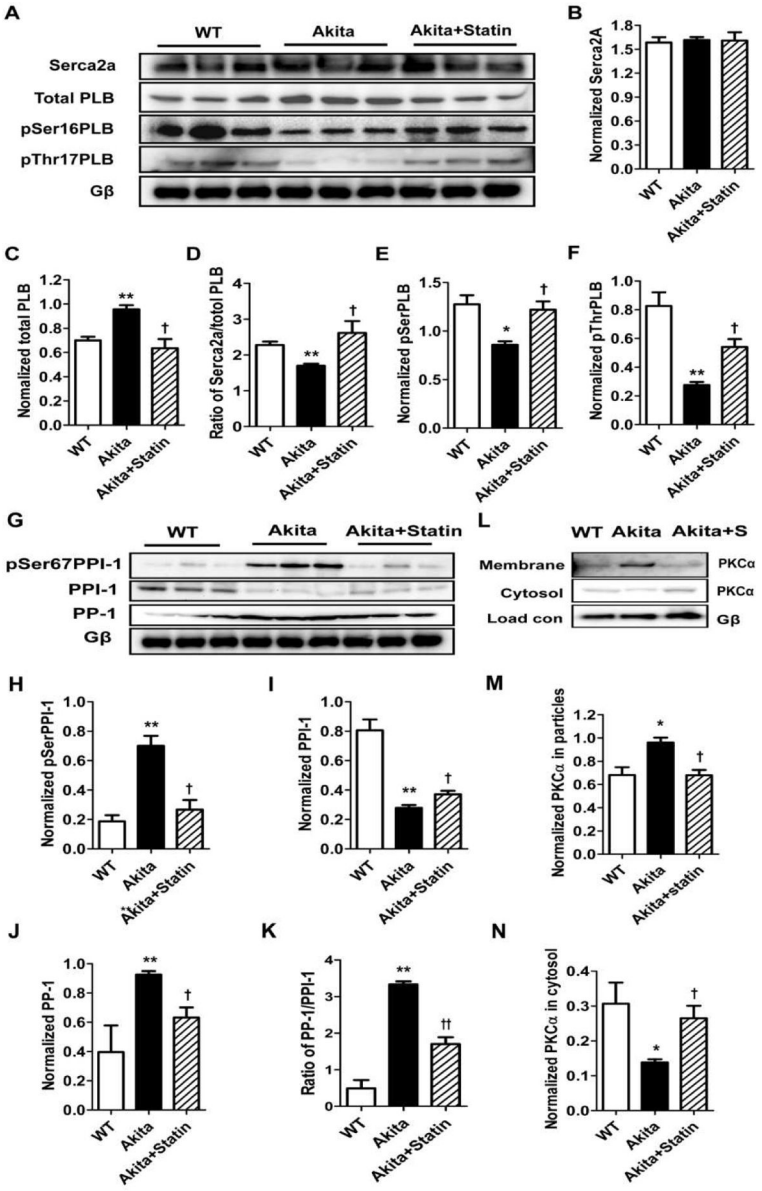

Figure 8.

Comparison of expression of major Ca^{2+} handling and PKCα proteins in ventricular extracts from WT, Akita and pravastatin treated Akitas. Western blotting demonstrates changes in protein levels among the 3 groups, A, G and L. Bar graphs represent data normalized to Gβ levels. **P*<0.05, ** *P*< 0.01 compared with WT; † *P*<0.05, ††*P*< 0.01 compared with Akita.